



Particle Acceleration due to Radiation Pressure in Relativistic Shock Waves

M. HOSHINO

University of Tokyo, Hongo, Bunkyo, Tokyo 113-0033, Japan

hoshino@eps.s.u-tokyo.ac.jp

Abstract: A particle acceleration by wakefield due to radiation pressure is discussed. For a relativistic shock with the upstream bulk Lorentz factor $\gamma_1 \gg 1$, the large-amplitude electromagnetic waves are generated in the shock front, and those waves can propagate into the upstream region as the precursor wave. We propose that non-thermal, high-energy particles can be quickly formed by the electrostatic wakefield generated by the ponderomotive force of the precursor wave. In the leading edge of the precursor wave, the particle can be quickly accelerated up to $\varepsilon \sim \gamma_1^2 m_e c^2$, and they can be further accelerated during the nonlinear evolution of the wakefield. The maximum attainable energy may be estimated by $\varepsilon \sim \gamma_1 m_e c^2 L_{sys} / (c/\omega_{pe})$, where L_{sys} and c/ω_{pe} are the size of an astrophysical object and the electron inertia length, respectively.

Introduction

After the discovery of cosmic ray in the early last century by the balloon experiments by Hess (1912), the origin of the cosmic rays have been a long standing problem. So far many acceleration process have been extensively studied, and the energies up to $10^{15.5}$ eV is believed to be generated by diffusive/Fermi acceleration mechanism operating in supernova shocks, but the cosmic rays with higher energies are not well understood yet (e.g., Hillas 1984).

Recently Chen et al.(2002) discussed a new idea of particle acceleration by “wave pressure” of large-amplitude Alfvén waves, and they proposed the origin of the ultra-high energy cosmic ray can be explained via the waves pressure. Their basic idea comes from the discovery of the wakefield acceleration in ultra-intense laser pulse (Tajima and Dawson 1979). By an action of the wave pressure of electromagnetic wave (photon), which is the so-called “ponderomotive force”, electrons are expelled from the intense electromagnetic wave pulse region, and then large-amplitude electrostatic wakefields are generated behind the packet of electromagnetic wave, which in turn can accelerate electrons and ions into relativistic energies (e.g., Esarey et al. 1996).

Recently the similar process of the wakefield is investigated by Lyubarsky (2006), who discussed energy conversion from ion to electron through large-amplitude electromagnetic waves generated in a relativistic shock upstream region. In this paper, we extend the intriguing study done by Lyubarsky, and demonstrate that high energy particles can be quickly generated by the electrostatic wakefields in association with the electromagnetic precursor waves in the relativistic shock.

Relativistic Shock Structure

We discuss the relativistic, ion-electron shock by using a one-dimensional, particle-in-cell (PIC) code. Shown in Figure 1 is a well-developed shock obtained by our simulation. We assumed that a low-entropy, relativistic plasmas consisting of electrons and ions is injected from the left-hand boundary. At the particle injection boundary, the plasma carries a uniform magnetic field B_z and a uniform motional electric field $E_y = v_x B_z / c$, polarized transverse to the plasma flow v_x . At the downstream right-hand boundary $x=0$, a wall where particles and waves are reflected is placed.

The x-axis is normalized by the electron relativistic inertia wavelength, $2\pi c/\omega_{pe}$, where the plasma

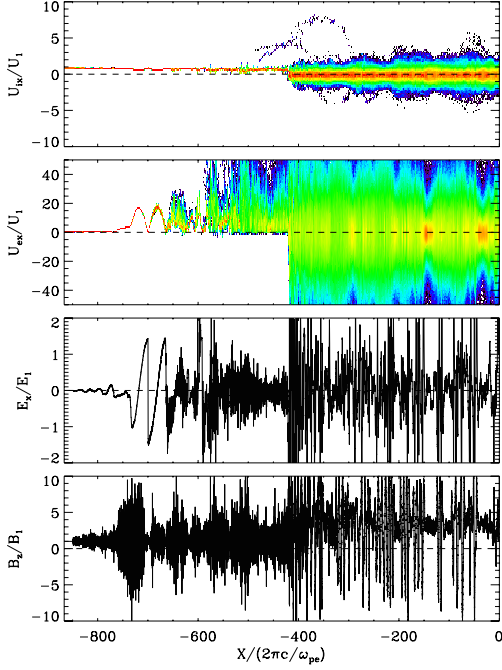


Figure 1: Relativistic shock structure. From the top, ion phase space U_{ix} , electron phase space U_{ex} , electric field E_x , and magnetic field B_z .

frequency $\omega_{pe} = \sqrt{4\pi N_1 e^2 / \gamma_1 m_e}$, the density N_1 in the simulation (shock downstream) frame. We also assumed that the speed of light $c=1$, the upstream bulk Lorentz factor $\gamma_1=10$ and the mass ratio of ion to electron $m_i/m_e=50$ in order to save the computational CPU time. The σ parameter is set to be $\sigma_{\text{total}} = B_1^2 / (4\pi N_1 \gamma_1 (m_i + m_e) c^2) = 2 \times 10^{-3}$ and $\sigma_e = B_1^2 / (4\pi N_1 \gamma_1 m_e c^2) \simeq 0.1$.

The snapshot in Figure 1 is obtained at $t\omega_{pe} = 5431$, and from the top, the ion phase space U_{ix} , the electron phase space U_{ex} , the longitudinal electric field E_x , and the transverse magnetic field B_z . These physical quantities are normalized by the corresponding upstream parameters. A shock front can be seen at the center of simulation box, i.e., $x/(2\pi c/\omega_{pe}) \sim -400$. The right-hand region corresponds to the shock downstream occupied by relativistic hot plasmas, while the left-hand region is the shock upstream/transition region with supersonic flows.

We can see that large amplitude electromagnetic (EM) waves (B_z) generated at the shock front are propagating into the shock upstream region. It has been discussed that the precursor EM waves are excited by the synchrotron maser instability at the shock front (Hoshino et al. 1992). The wave energy density $B_1^2/8\pi$ is about 10% – 100% of the upstream electron bulk flow energy density $N_1 \gamma_1 m_e c^2$. At the time of $t\omega_{pe} = 5431$, the tip of the precursor waves reached at $x/(2\pi c/\omega_{pe}) \sim -850$, and we obtain that the propagation velocity of the precursor wave is about $(850 \times 2\pi c)/5431 \sim 0.98c$, which is almost equal to the speed of light. In contrast with non-relativistic shock waves, the relativistic shocks can transfer a large amount of energy into not only the lower frequency MHD waves but also the higher frequency electromagnetic waves.

Associated with the precursor wave, the generation of large-amplitude electrostatic wakefields E_x and the electrons heating and acceleration become significant. In the leading edge of the precursor wave B_z , sinusoidal structures can be recognized for both the wakefields E_x and the modulation of the electron phase space U_{ex} . As approaching toward the shock front, those waves start to collapse and strong plasma scattering and acceleration occurs. The energy of the accelerated electrons reach up to more than $\varepsilon/m_e c^2 \sim 50$, which is larger than the upstream bulk flow energy of ions $\gamma_1 m_i c^2$.

Particle Acceleration by Wakefields

As we can observe in our simulation result, electrons are thermalized/accelerated in association with the electromagnetic precursor waves B_z and the electrostatic wakefields E_x . The good correlation between the electron phase space U_{ex} and the electric field E_x can be clearly seen around $x/(2\pi c/\omega_{pe}) \sim 700$. This is suggestive that those electrons gain energy from the wakefields E_x .

The energy gain of charge particles in astrophysical settings is believed to be evaluated by $\varepsilon \sim eEL$, where E and L are the motional electric field $v \times B/c$ and the scale size of system, respectively (e.g. Hillas 1984). Our point in this paper is that the electric field E is given by the wakefield E_x , which

magnitude is large than the motional electric field $E = vB/c$.

Let us first estimate the wakefield amplitude, which is generated by an action of the ponderomotive force of the precursor wave. The origin of the ponderomotive force can be understood as “wave pressure” under the interaction of charge particles and the coherent wave (e.g., Kruer 1988). The ponderomotive force F_{pond} is expressed by $F_{\text{pond}} = -e\nabla\phi_{\text{pond}}$, where the generalized ponderomotive potential $\phi_{\text{pond}} = m_j c^2 \sqrt{1 + a_0^2}$ (e.g., Bauer et al. 1995), the normalized amplitude $a_0 = eE_0/m_j c \omega_0$. $j = i, e$ stands for either ion or electron. Since the electron ponderomotive force is much larger the ion one, electrons are expelled from the large amplitude wave region, and then the polarization electrostatic field is generated in order to maintain the charge neutrality in plasma. Then the induced electrostatic field initiates the plasma oscillation behind the precursor waves. This is a basic mechanism of “wakefield”.

Based on the simulation study of the pair plasma shock (Gallant et al. 1992), the amplitude of EM precursor wave E_0 can be estimated as $E_0/B_1 \sim (\epsilon_{\text{conv}}/\sigma_e)^{1/2}$, where B_1 is the upstream magnetic field and $\epsilon_{\text{conv}} \sim O(1)$ is the energy conversion rate from the upstream bulk energy into the precursor wave energy. The precursor frequency ω_0 is also known to be $\omega_0/\omega_{pe} \sim 2 - 3$. Then we can obtain the normalized amplitude $a_0 \sim \gamma_1 \sqrt{\epsilon_{\text{conv}}}$. From the above, we can obtain the amplitude of the wakefields as

$$E_{\text{wake}}/B_1 \sim \sigma_e^{-1/2}. \quad (1)$$

Next we investigate the scale length of the wakefield. An interaction of the electromagnetic (EM) wave (i.e., precursor wave) and the Langmuir wave (i.e., wakefield) through the ponderomotive force can be understood by the so-called Raman scattering process in plasma (e.g., Mima and Nishikawa 1988). When the frequency and wave number of the pump EM wave is given by (ω_0, k_0) , the scattering EM wave with (ω_1, k_1) and the induced Langmuir wave with (ω_2, k_2) have to satisfy the wave-wave coupling conditions of $\omega_0 = \omega_1 + \omega_2$ and $k_0 = k_1 + k_2$. Note that the wave dispersion relations of EM mode $\omega_j^2 = k_j^2 c^2 + \omega_{pe}^2$ for $j = 0, 1$ and of Langmuir mode $\omega_2 = \omega_{pe}$ should be also satisfied. For the case of $\omega_0 \gg \omega_{pe}$,

we can easily find that the Langmuir wave has $(\omega_2, k_2) \sim (\omega_{pe}, \omega_{pe}/c)$ in proper frame where the ambient plasma is at rest (e.g., Kruer 1988).

Due to Lorentz transformation of the Langmuir wave, we obtain the wave length of the wakefield L_{wake} in the laboratory (shock downstream) frame,

$$L_{\text{wake}} \sim 2\gamma_1 c/\omega_{pe}. \quad (2)$$

This estimation gives a good agreement with the wakefield structure observed at the tip of the precursor in Figure 1.

From Eqs.(1) and (2), the energy gain in the sinusoidal precursor region can be estimated by

$$\varepsilon \sim eE_{\text{wake}}L_{\text{wake}} \sim \gamma_1^2 m_e c^2. \quad (3)$$

By comparing the above theory with the simulation result in Figure 1, we find the theory can correctly predict the modulation energy of the electron phase space in the leading edge of the wakefields around $x/(2\pi c/\omega_{pe}) \sim -700$.

We now discuss the most important acceleration process behind the sinusoidal wakefield region. In the turbulent wakefield region, we think that a successive Raman scattering process is happening. Namely, the scattered EM (daughter) wave due to the Raman process may decay again into another scattered EM (grand-daughter) wave and another Langmuir wave. This nonlinear Raman process may continue as long as the frequency of the decay EM wave is larger than the plasma frequency ω_{pe} . During this Raman process, a broadband wave spectrum can be generated.

If we observe the lower frequency part of the broadband spectrum in the shock downstream frame, they can propagate into the downstream direction due to the Doppler shift effect. Then we may expect the stochastic particle acceleration with a random acceleration-decelerating phase inside the turbulent wakefield region. The important point is that a particle can resonance with the wave propagating toward downstream. Therefore, we may estimate the maximum attainable energy in the turbulent wakefields by

$$\varepsilon \sim eE_{\text{wake}}L_{\text{sys}}\epsilon_{\text{eff}} \sim \gamma_1 m_e c^2 \frac{L_{\text{sys}}}{c/\omega_{pe}} \epsilon_{\text{eff}}, \quad (4)$$

where L_{sys} and ϵ_{eff} denote the region size of the wakefields and the efficiency the stochastic acceleration. The system size L_{sys} may be roughly

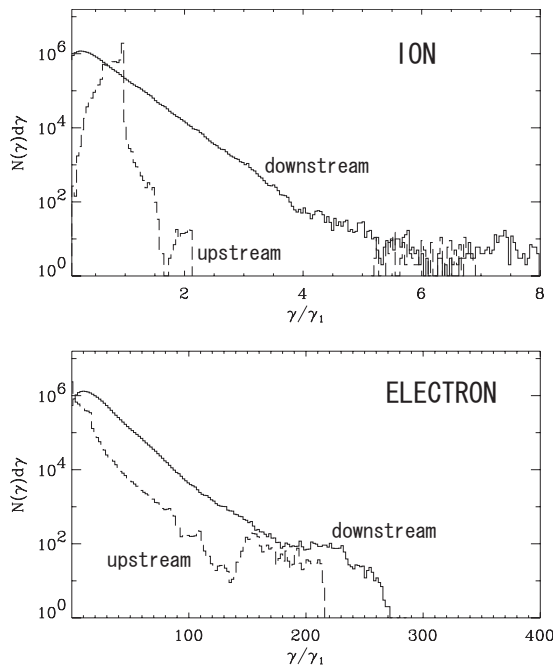


Figure 2: Energy spectra for ions and electrons

estimated from the difference of the propagation speeds between the precursor wave and the shock wave, i.e., $L_{\text{sys}} \sim ct(1 - \sqrt{\Gamma - 1})$, where Γ is the ratio of the specific heat. By comparing Eq.(4) with the time history of the maximum energy obtained in our simulation (not shown here), we numerically obtained $\epsilon_{\text{eff}} \sim 1/6 - 1/3$. This efficiency is better than our expectation, and such a good efficiency seems to be due to the shock surfing acceleration process near the shock front (e.g., Hoshino and Shimada 2002).

Conclusions and Discussion

We discussed that the wakefields provide high-energy particle acceleration through the large-amplitude electromagnetic precursor waves. So far we mainly investigated electron acceleration, but we think that the wakefield acceleration is equally important for ion acceleration. Shown in Figure 2 is the energy spectra for ions and electrons. The upstream and the downstream spectrum are denoted by the dashed and the solid line, respectively. We find that electrons are already accelerated up to

$\epsilon/\gamma_1 m_e c^2 \sim 215$ in upstream, and the maximum energy is almost same as the downstream energy. Ions also show the similar behavior to electrons, and the maximum energy is about $\epsilon/\gamma_1 m_i c^2 \sim 8$, which is of the same order of the electron maximum energy, because the mass ratio of ion to electron is assumed to be 50 in our simulation.

Our simulation study is only a first step to understanding the potential rich wakefield acceleration. It is important to study further our simple acceleration process from several other aspects: one is the radiation loss process such as the synchrotron loss and Compton scattering. Another is the wave coherency of the precursor wave that is probably the most important issue, because the coherency is required for the ponderomotive force. Otherwise the effect of the radiation pressure force enters into the standard Thomson scattering regime.

Acknowledgements

This work is partially supported by Grand-in-Aid for Science Research-B. The computation was done by NEC/SX-6 at ISAS/JASA computer center.

References

- [1] Bauer, D. et al. 1995, PRL, 75, 4622
- [2] Chen, P. et al. 2002, PRL, 90, 161101
- [3] Esarey, E., Sprangle, P., Krall, J., & Ting, A. 1996, IEEE Trans. Plasma Sci., 24, 252
- [4] Gallant, Y. A. et al. 1992, ApJ, 391, 73
- [5] Hess, V., 1992, Physik. Zeitschr., 13, 1084
- [6] Hillas, A. M., 1984, Ann. Rev. Astron. Astrophys. 22, 425
- [7] Hoshino, M. et al. 1992, ApJ, 390, 454
- [8] Hoshino, M. & Shimada, N., 2002, ApJ, 572, 880
- [9] Kruer, W. L., 1988, The Physics of Laser Plasma Interaction, Addison-Wesley Publ.
- [10] Lyubarsky, Y. E., 2006, ApJ, 652, 1297
- [11] Mima, K. & Nishikawa, K. 1988, Parametric Instabilities and Wave Dissipation in Plasmas, in Basic Plasma Physics, eds. M.N. Rosenbluth and R.Z. Sagdeev, North-Holland Phys. Publ.
- [12] Tajima, T., & Dawson, J.M. 1979, PRL, 23, 267